Author's personal copy

Current Applied Physics 12 (2012) 105–108

Contents lists available at ScienceDirect

Current Applied Physics

journal homepage: www.elsevier.com/locate/cap

Breakthrough/drainage pressures and X-ray water visualization in gas diffusion layer of PEMFC

Jongrok Kim [a], Junho Je [a], TaeJoo Kim [b], Massoud Kaviany [c], Sang Young Son [d], MooHwan Kim [e,*]

[a] Department of Mechanical Engineering, Pohang University of Science and Technology, San 31, Hyoja-dong, Namgu, Pohang, Kyoungbuk 790-784, Republic of Korea
[b] The Korea Atomic Energy Research Institute, 150 Deokjin-dong, Yuseong-gu, Daejeon 305-353, Republic of Korea
[c] Department of Mechanical Engineering, University of Michigan, Ann Arbor, MI 48109-2125, USA,
[d] School of Dynamic Systems, University of Cincinnati, Cincinnati, OH 45221, USA
[e] Division of Advanced Nuclear Engineering, Pohang University of Science and Technology, San 31, Hyoja-dong, Namgu, Pohang, Kyoungbuk 790-784, Republic of Korea

ARTICLE INFO

Article history:
Received 16 November 2010
Received in revised form
19 April 2011
Accepted 7 May 2011
Available online 25 May 2011

Keywords:
Break-through pressure
Drainage pressure
Gas diffusion layers
Polymer electrolyte membrane fuel cell
X-ray tomography

ABSTRACT

The primary role of the gas diffusion layers (GDLs) in polymer electrolyte membrane fuel cells (PEMFC) is to maintain the delicate balance between water retention and removal in GDLs. Water management in the fuel cell is related to the breakthrough pressure at which water starts to pass through GDL, and the drainage pressure, which is maintained after the breakthrough. These pressures are both related to water management in fuel cells. Here we measured these pressures for two different GDLs and used X-ray tomography to visualize the water distributions within them. We then relate the variations in liquid pressures to the visualization and discuss water management in PEMFC.

© 2011 Elsevier B.V. All rights reserved.

1. Introduction

A fuel cell is an electrochemical device that converts the bond energy of reactants directly to electricity. PEMFC, which uses a soft-matter proton-conducting polymer membrane as the electrolyte, produces water and this water either remains in the pores of the gas diffusion layer (GDL) and membrane or leaves the fuel cell. Management of the pore water is required to maintain appropriate water content in the electrolyte phase and to ensure proton transport through it, while avoiding flooding, which hinders the transport of reactants by filling the pores in the GDL and by covering catalytic reaction sites. Failure to do this results in a significant reduction in cell performance and durability [1,2]. Because pore water content is directly influenced by the GDL structure, understanding water distribution in the GDL is important.

Many studies have examined two-phase transport in PEM fuel cells using constitutive relationships for liquid water flow in the porous layers. Two approaches exist for modeling the liquid water behavior in PEM fuel cells. The first is the macroscopic PEM fuel cell model, based on the two-phase Darcy law under assumptions of a homogeneous pore structure and uniform wetting characteristics [3–6]. The second approach is pore-scale modeling and simulation, which is based on a more precise investigation of the liquid water transport mechanism through a fibrous diffusion media (DM) structure [7,8]. These approaches use the capillary pressure in a GDL as an important parameter in analyzing water transport. However, the capillary pressure from analytic equations has limitations in modeling the characteristics of real-life GDLs, because GDL carbon fibers have heterogeneous surfaces and structures. The breakthrough pressure [9,10] and the drainage pressure can be used to represent GDL characteristics. These pressures are strongly related to the water distribution in a GDL. In this study, the water distributions in GDLs with and without the microporous layers (MPLs) were visualized with the X-ray tomography, which was employed to visualize the water transport in the PEM fuel cells. Previous studies [11–15] have also used the X-ray imaging, here we used the X-ray microscope at the Pohang Accelerator Laboratory in Korea to

* Corresponding author. Tel.: +82 54 279 2165; fax: +82 54 279 3199.
E-mail addresses: jongrok@postech.ac.kr (J. Kim), sofujuno@postech.ac.kr (J. Je), tj@kaeri.re.kr (TaeJoo Kim), kaviany@umich.edu (M. Kaviany), sangyoung.son@uc.edu (S.Y. Son), mhkim@postech.ac.kr (MooHwan Kim).

1567-1739/$ – see front matter © 2011 Elsevier B.V. All rights reserved.
doi:10.1016/j.cap.2011.05.016

Author's personal copy

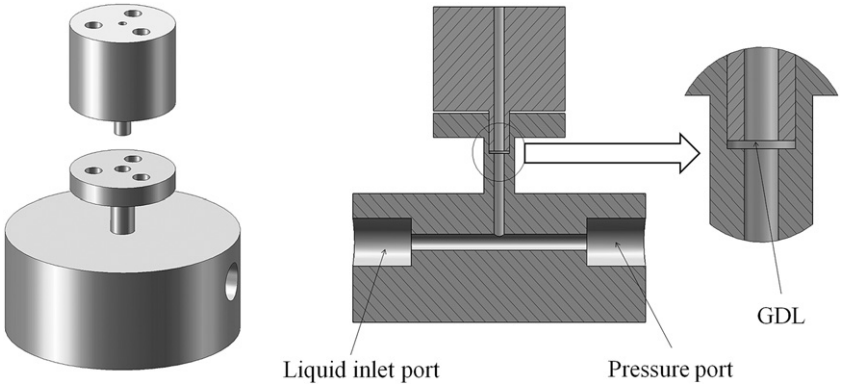

Fig. 1. GDL housing for measurement of capillary pressure.

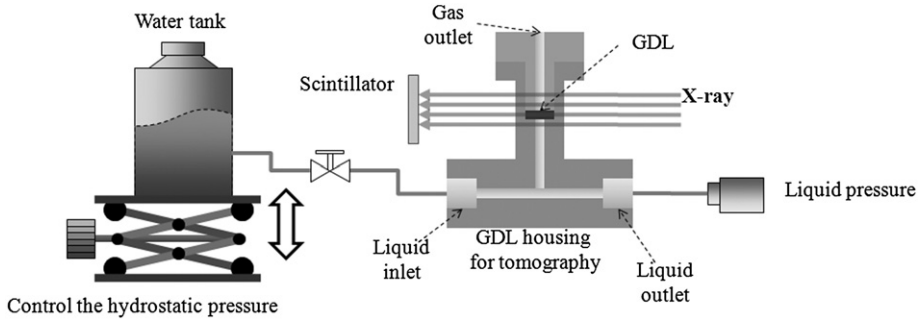

Fig. 2. Schematic diagram of experimental apparatus. The liquid inlet port is connected to the pressurized water. The liquid outlet, air inlet, and outlet ports were exposed to ambient air.

transient observations and the accompanying measurement of the breakthrough and the drainage pressures.

2. Experiment and discussion

An experimental system was designed to visualize GDLs with X-rays while measuring the liquid pressures. As shown in Fig. 1, a GDL housing consisting of two cylindrical blocks was used to enclose a GDL. Pressurized water was supplied to bottom of the GDL and the water pressure was measured with a pressure transmitter as shown in Fig. 2. The experiments were performed at the 7B2 X-ray Microscopy Beamline of the Pohang Accelerator Laboratory. The X-ray beam from a bending magnet was created with dimensions 120 (horizontal) $\times$ 45 (vertical) μm^2 with the microscopy system located at a distance of 34.8 m. The beam angular divergences were 8.3 μrad (vertical) and 20 μrad (horizontal), and the beam strengths were 2.8 keV at 2 GeV/5.5 keV at 2.5 GeV. The X-ray beam was directed through the sample to a 150 μm $CdWO_4$ scintillator that converted the X-rays to visible beam. This visible beam reflected off a mirror into a 4008 $\times$ 2672-pixel charge-coupled-device camera through a microscope. The field of view was 5.05 $\times$ 3.36 mm^2.

The typical experimental process was as follows:

1) Supply pressurized water through liquid inlet.
2) Close the liquid inlet valve when the liquid pressure reaches the hydrostatic pressure.
3) Record X-ray images of the test section while the liquid pressure is at steady state.
4) Repeat steps 1–3.

The first experiment was done with an untreated Toray TGPH-090 GDL. In step 3 of the experimental process, the liquid pressure decreased until it reached steady state (Fig. 3). The reason for this behavior is that the supplied water needed time to diffuse fully in the GDL. As the experimental processes were repeated, the liquid pressure increased to the breakthrough pressure P_1 (Fig. 3). Breakthrough occurred at pressures above P_1, and the liquid pressure decreased dramatically to almost zero. The liquid pressure did not drop completely to zero after breakthrough because the water that passed through the GDL into the gas outlet hole increased the

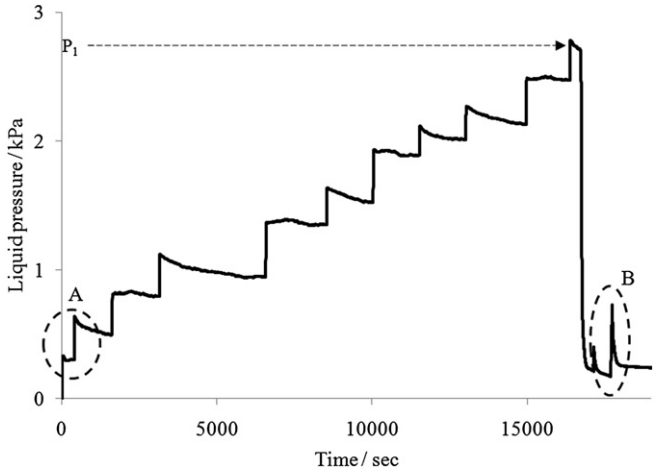

Fig. 3. Liquid pressure for the Toray TGPH-090 GDL.

Author's personal copy

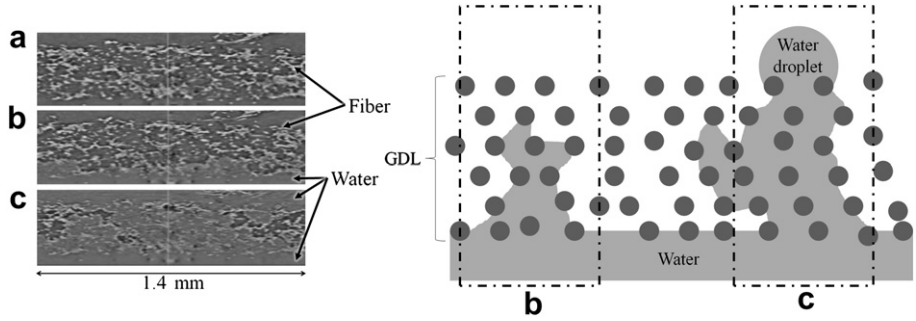

Fig. 4. The X-ray tomography and the simplified model results for GDL water distribution of the untreated TGPH-090, (a) before water injection, (b) at less than 2.13 kPa, and (c) after the breakthrough.

hydrostatic pressure. The liquid inlet valve was then opened to increase the liquid pressure again. In this case, the liquid pressure also decreased dramatically (region B in Fig. 3) to near zero, in contrast to region A (Fig. 3) where the liquid pressure remained constant.

This difference between regions A and B can be explained by X-ray tomography water visualization and the simplified model (Fig. 4). Before the liquid pressure reached P_1, the percolated water could not form a complete water column from the liquid side to the other side of the GDL. Thus, capillary force, which prevented water movement, affected the head of the water column. Otherwise, after the liquid pressure reached P_1, the water column connected both sides of the GDL and the capillary force at the head of the water column vanished. For this reason, after the liquid pressure reached P_1, water could readily move up through the water column under low pressure conditions, whereas it could not move up before the liquid pressure reached P_1. This indicates that this GDL easily vented water after breakthrough.

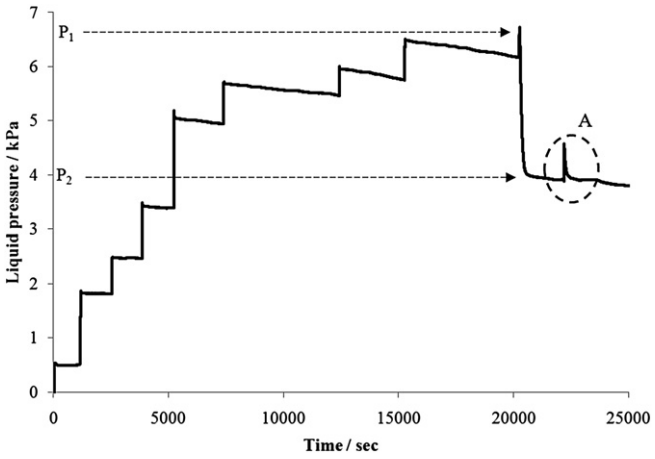

Fig. 5. Liquid pressure for the SGL 10BB GDL.

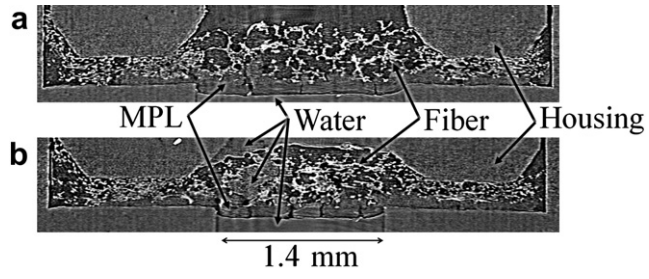

Fig. 6. Water distribution in the GDL of the bare SGL 10BB (a) at less than 6.2 kPa and (b) after breakthrough.

The experiment was repeated with an SGL 10BB GDL, which was made by applying a MPL coating to a 10BA GDL (Fig. 5). In this case, the breakthrough pressure was greater than that of the TGPH-090 GDL, even though previous research reported that 10BA has a lower capillary pressure than the TGPH-090 according to the pressure–saturation relationship [16]. Above P_1, the liquid pressure also decreased, but the decrease stabilized at a certain pressure (P_2, the drainage pressure) while the liquid pressure of the TGPH-090 after breakthrough decreased to almost zero. In the visualization of the water distribution in 10BB, no water was observed in the fiber structure of the GDL before breakthrough and percolated water existed in the fiber structure of GDL after breakthrough (Fig. 6). This result contrasts with the case of the TGPH-090 in that some water percolated into the GDL before breakthrough. After water passed through the MPL, its pressure was higher than the breakthrough pressure of the GDL fiber structure because the MPL had a higher capillary pressure than that of the GDL. Thus, the breakthrough in the whole GDL occurred after breakthrough in the MPL, and water was observed in the fiber structure. To maintain the liquid pressure after breakthrough (P_2), we suggest that the water column formed was broken in the MPL below the drainage pressure, because the water could not attach to the surface of the hydrophobic particles of the MPL. These behaviors of pressure indicate that the MPL is the dominant factor in the water behavior in GDLs and is a useful tool for maintaining the hydrated condition of the membranes in operating fuel cells where flooding often occurs.

3. Conclusions

In this study, the liquid water pressures in two different GDLs are measured and analyzed using X-ray tomography of the water distribution. The liquid pressure in TGPH-090 GDL dramatically vanishes after the breakthrough, since a complete water column is formed when the breakthrough occurs. In the case of the 10BB, the breakthrough pressure is larger, even though 10BA has a lower capillary pressure. Moreover, the decrease in liquid pressure after the breakthrough stabilizes at a nonvanishing drainage pressure. These results demonstrate that the MPL controls the water behavior in GDLs and is a useful tool for controlling the humidity in PEMFC.

Acknowledgments

This research was supported by WCU (World Class University) program through the National Research Foundation of Korea funded by the Ministry of Education, Science and Technology and the

Author's personal copy

National Research Foundation of Korea (NRF) through a grant provided by the Korean Ministry of Science and Technology (MOST), (M60602000005-06E0200-00410).

References

[1] J. Larminie, A. Dicks, Fuel Cell Systems Explained, second ed. Wiley, West Sussex, 2003, p.70.
[2] G.A. Eisman, The application of Dow chemical's perfluorinated membranes in proton exchange membrane fuel cells, J. Power Sources 29 (1990) 389–398.
[3] J.H. Nam, M. Kaviany, Effective diffusivity and water-saturation distribution in single- and two-layer PEMFC, International Journal of Heat and Mass Transfer 46 (2003) 4595–4611.
[4] Z.H. Wang, C.Y. Wang, K.S. Chen, Two phase flow and transport in the air cathode of proton exchange membrane fuel cells, J. Power Sources 94 (2001) 40–50.
[5] S. Mazumder, J.V. Cole, Rigorous 3-D mathematical modeling of PEM fuel cells II. Model predictions with liquid water transport, Journal of the Electrochemical Society 150 (11) (2003) A1510–A1517.
[6] L. You, H. Liu, A two-phase flow and transport model for the cathode of PEM fuel cells, International Journal of Heat and Mass Transfer 45 (2002) 2277–2287.
[7] T. Koido, T. Furusawa, K. Moriyama, An approach to modeling two-phase transport in the gas diffusion layer of a proton exchange membrane fuel cell, J. Power Sources 175 (2008) 127–136.
[8] P.K. Sinha, C.Y. Wang, Liquid water transport in a mixed-wet gas diffusion layer of a polymer electrolyte fuel cell, Chem. Eng. Sci. 63 (2008) 1081–1091.
[9] J. Benziger, J. Nehlsen, D. Blackwell, T. Brennan, J. Itescu, Water flow in the gas diffusion layer of PEM fuel cells, Journal of Membrane Science 261 (2005) 98–106.
[10] J.T. Gostick, M.A. Ioannidis, et al., On the role of the microporous layer in PEMFC operation, Electrochemistry Communications 11 (3) (2009) 576–579.
[11] I. Manke, C. Hartnig, M. Grunerbel, W. Lehnert, N. Kardjilov, A. Haibel, A. Hilger, J. Banhart, H. Riesemeier, Investigation of water evolution and transport in fuel cells with high resolution synchrotron x-ray radiography, Applied Physics Letters 90 (17) (2007) 174105.
[12] F.N. Büchi, R. Flückiger, D. Tehlar, F. Marone, M. Stampanoni, Determination of liquid water distribution in porous transport layers, ECS Transactions 16 (2008) 587–592.
[13] J. Becker, R. Flückiger, M. Reum, F.N. Büchi, F. Marone, M. Stampanoni, Determination of material Properties of gas diffusion layers: experiments and simulations using phase contrast tomographic microscopy, Journal of the Electrochemical Society 156 (2009) B1175–B1181.
[14] T. Sasabe, S. Tsushima, S. Hirai, In-situ visualization of liquid water in an operating PEMFC by soft X-ray radiography, International Journal of Hydrogen Energy 35 (2010) 11119–11128.
[15] Z. Fishman, J. Hinebaugh, A. Bzylak, Microscale tomography investigations of heterogeneous porosity distributions of PEMFC GDLs, Journal of the Electrochemical Society 157 (11) (2010) B1643–B1650.
[16] J.T. Gostick, M.W. Fowler, M.A. Ioannidis, M.D. Pritzker, Y.M. Volfkovich, A. Sakars, Capillary pressure and hydrophilic porosity in gas diffusion layers for polymer electrolyte fuel cells, Journal of Power Sources 156 (2006) 375–387.